EUROPEAN ORGANIZATION FOR NUCLEAR RESEARCH

Proposal to the ISOLDE and Neutron Time-of-Flight Committee

Characterization of the low-lying 0^+ and 2^+ states of ^{68}Ni

September 25, 2013

C. Sotty[1], P. Van Duppen[1], M. Huyse[1], L.M. Fraile[2], A. Algora[3], A. Andreyev[4], M.L.L. Benito[5], S. Bönig[6], C. Borcea[7], R. Borcea[7], B. Cheal[8], T.E. Cocolios[9], H. De Witte[1], H. Duckwitz[10], P. Fernier[5], F. Flavigny[1], L. Gaffney[1], T. Grahn[11,12], P.T. Greenless[11,12], S. Ilieva[6], J. Jolie[10], R. Julin[11,12], U. Koester[13], T. Kröll[6], R. Lica[7], H. Mach[15], N. Mărginean[7], R. Mărginean[7], C. Mihai[7], F. Negoita[7], A. Negret[7], B. Olaizola[2], R. Page[8], J. Pakarinen[11,12], S. Pascu[7], V. Paziy[2], E. Piselli[5], D. Radulov[1], E. Rapisarda[5], F. Rotaru[7], M. Stanoiu[7], O. Tenglad[14], T. Thomas[10], M. Thürauf[6], J.M. Udías[2], V. Vedia[2], D. Voulot[5], W.B. Walters[16], N. Warr[10], F. Wenander[5].

[1] *Instituut voor Kern- en Stralingsfysica, K.U. Leuven, Leuven, Belgium*
[2] *Universidad Complutense, Madrid, Spain*
[3] *Instituto de Fisica Corpuscular, University of Valencia, Valencia, Spain*
[4] *Department of Physics, University of York, Heslington, UK*
[5] *ISOLDE, CERN, Geneva, Switzerland*
[6] *Institut fuer Kernphysik, Technische Universitaet Darmstadt, Darmstadt, Germany*
[7] *"Horia Hulubei" National Institute for Physics and Nuclear Engineering, 077125 Bucharest-Magurele, Romania*
[8] *University of Liverpool, Liverpool, UK*
[9] *University of Manchester, Manchester M13 9PL, Lancashire, United Kingdom*
[10] *Institut fuer Kernphysik, Universitaet zu Koeln, Koeln, Germany*
[11] *Department of Physics, University of Jyväskylä, Jyväskylä, Finland*
[12] *Helsinki Institute of Physics, Helsinki, Finland*
[13] *Institut Laue-Langevin, Grenoble, France*
[14] *Instituto de Estructura de la Materia, Madrid, Spain*
[15] *BP1, NCBJ - National Center for Nuclear Research, Otwock, Poland*
[16] *Department of Chemistry, University of Maryland, Maryland, USA*

Spokespersons: C. Sotty[*Christophe.Sotty@fys.kuleuven.be*], L. M. Fraile[*luis.fraile@cern.ch*]
Contact person: E. Rapisarda [*Elisa.Rapisarda@cern.ch*]

Abstract:
Recently, a number of low-lying low-spin states have been firmly identified in ^{68}Ni; the position of the first excited state (which is a 0^+ state), the spin and parity of the second excited 0^+ state and the spin and parity of the second and third 2^+ states have been fixed. The identification of these three pairs of 0^+ and 2^+ states in ^{68}Ni (Z=28 and N=40) forms ideal tests to validate shell-model calculations and the effective interactions developed for the nickel region but also hints to triple shape coexistence including even strongly deformed structures. The aim of this proposal is to collect detailed spectroscopic data of the low-spin states of ^{68}Ni (Z=28, N=40) in order to characterize these triple pairs of 0^+ and 2^+ states. Gamma branching ratios of the 0^+ and 2^+ states and the E0 transition strengths as well as the E2 transition rate of the 0_3^+ will be obtained using the new ISOLDE Decay Station that is constructed from an efficient array of germanium detectors and further equipped with high resolution electron. The IDS germanium array will be supplemented with fast-timing detectors and high resolution electron detectors to determine the half-life of 0_3^+ states and the E0(0^+-0^+) decay branches. The low-spin states in ^{68}Ni will be populated in β decay of the low-spin isomer in ^{68}Co($T_{1/2}$=1.6 s), which will be produced by the decay of ^{68}Mn laser-ionized by RILIS.

Requested shifts: [28] shifts, (split into [2] runs over [1] years)

CERN-INTC-2013-051 / INTC-P-402
02/10/2013

1 Introduction: Magicity versus collectivity in and around ^{68}Ni

According to the shell model the Z=28 is a magic number while the N=40 shell-gap is qualified as a semi-magic sub-shell. The term of sub-shell is employed to indicate that the effects of the shell-closure should be less pronounced due to a smaller energy gap between the single-particle orbitals. In this prescription, ^{68}Ni with Z=28 and N=40 is classified as a semi-doubly magic nucleus. The structure of ^{68}Ni and of the neighboring nuclei makes this region particularly interesting for testing the shell-model, the validity of the magic numbers and the onset of collectivity.

In the particular case of the Ni isotopic chain, the energy of the first excited 2^+ state reaches a maximum at N=40 (E=2.033 MeV) [1] and a minimum for the B(E2;$2_1^+ \rightarrow 0_1^+$)=3.2(7) W.u. [2], which is in sharp contrast with the neighboring even-even isotopes. Moreover, the first 0^+ state has been reported at 1.7 MeV [3], lower than the first 2^+ state at 2033 keV. The inversion of the 2_1^+ and 0_2^+ mimics the doubly magic ^{40}Ca or ^{16}O nuclei, see Ref. [3, 4]. These observations led to a discussion on the possible manifestation of semi-magicity of the N=40 neutron sub-shell. However, mass measurements do not show a pronounced energy gap at N=40. Furthermore, the removal of valence nucleons from the ^{68}Ni core to lighter iron and chromium isotopes leads to a sudden increase of deformation as deduced from the trends of E(2_1^+) and B(E2;$2_1^+ \rightarrow 0_1^+$) values. Also β-decay studies of the neighboring odd-A nuclei showed a significant polarization of the ^{68}Ni core nucleus when coupling nucleons, which implies a rapid decrease in the stabilizing effect of N=40 [5–7].

This apparent contradiction, between collective and magic features, has triggered different theoretical studies, see Ref. [4, 8–18]. Some of the theoretical studies predict the presence of different low-lying 0^+ states in ^{68}Ni, explained via different scenarios, such as the appearance of a proton intruder 0^+ state [18]. For example, the Q-constrained Hartree-Fock calculation on ^{68}Ni, performed by Y. Tsunoda *et al.* [13], provides the total energy surface shown on Fig. 1.

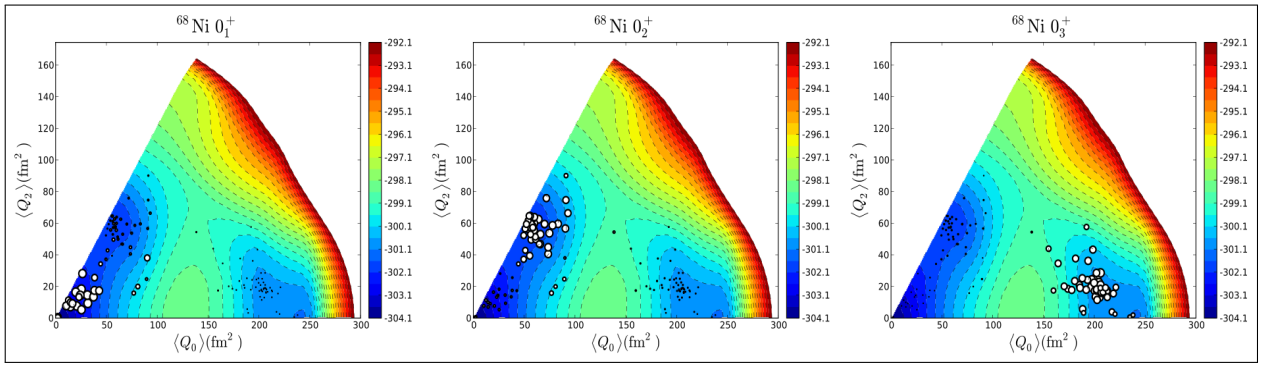

Figure 1: Total energy surface of the 0_1^+ (left), 0_2^+ (middle) and 0_3^+ (right) states of ^{68}Ni. The positions of the red circles represent quadrupole deformations of the MCSM basis states before projection. The areas of those circles represent the overlap probabilities of the basis states and the resulting wave function. Based on Ref. [13].

The projection of the 0^+ states predicts a spherical-like shape for the 0_1^+ state, and an oblate deformation for the 0_2^+ state. A third minimum corresponding to a strongly prolate shape is also present and it is advocated that the third 0^+ state in ^{68}Ni is situated in this minimum [12, 13, 19].

Shell model calculations using the LNPS interaction have been performed for ^{68}Ni by Lenzi *et al.* [17], and are presented in the thesis of A. Dijon [20]. This interaction is one of the most recently developed and reproduces well the deformation in the Cr isotopic chain (interpreted as the consequence of the π-ν correlation energy between the neutron $g_{9/2}$, $d_{5/2}$ shells and proton pf orbitals). Quasi-particle Random Phase Approximation (QRPA) calculations with the D1S interaction for ^{68}Ni, presented in the thesis of A. Dijon [20] predict an excited 0^+ state at 2.24 MeV. Both the shell model and the QRPA calculations predict a 0^+ isomeric state (at 2.4 MeV and 2.24 MeV respectively) at around the same energy as the proton-intruder state predicted by D. Pauwels *et al.* [18]. The shell-model calculations indicate a strongly deformed character for the 0_3^+ state.

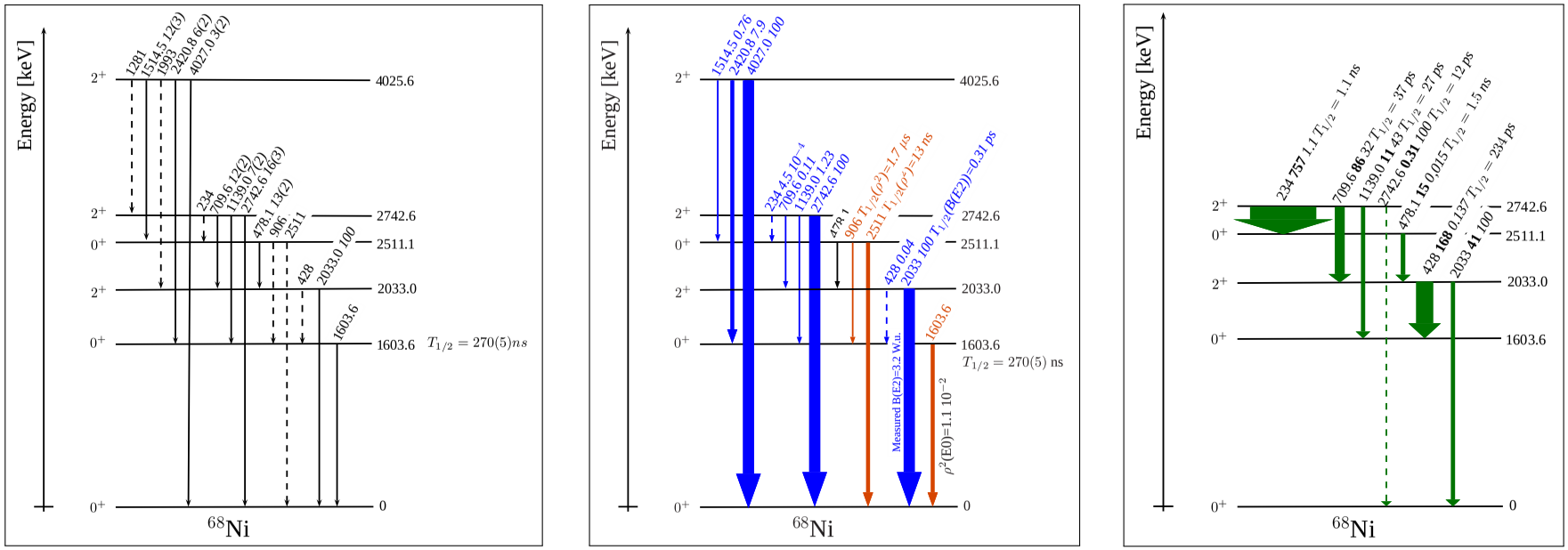

Figure 2: Partial level schemes of the low-lying 0^+-2^+ states of ^{68}Ni.
(a) From the decay study [21]. The observed E0 and E2 transitions are represented with full arrows, the other transitions by dashed arrows. The labeling of the transitions corresponds to the following pattern: E_γ [keV], relative intensity [%] to the 2033.0 keV 2_1^+-0_1^+ transition.
(b) Calculation of the relative intensities of the different transitions, purely based on their E2 (blue) or E0 (brown) character and assuming identical B(E2) values or the same $\rho^2(E0)$ value as deduced from the 0_2^+-0_1^+ transition respectively. The labeling of the transitions corresponds to the following pattern: E_γ [keV], relative intensities. The partial half-life of the 2033.0 keV transition has been deduced from its measured B(E2) transition strength [2]. The monopole density strength $\rho^2(E0)$ of the 1603.6 keV transition is derived from its measured energy and half-life of 270(5) ns [2]. The partial half-lives of the 2511 keV and 906 keV E0 transitions have been determined based on the $\rho^2(E0)$ of the 1603.6 keV transition.
(c) Relative γ-ray intensities using the theoretical $B(E2,\downarrow)^{theo.}$ values reported in [20] and based on the LNSP calculations. The labeling of the transitions corresponds to the following pattern: E_γ [keV], $B(E2,\downarrow)^{theo.}$ [$e^2.fm^4$] transition strengths, relative intensity ratios assuming pure E2 transitions and partial half-lives deduced from the $B(E2,\downarrow)^{theo.}$.

2 Present experimental evidence

Next to important experimental work at MSU, ANL and GANIL, also at ISOLDE ^{68}Ni and its neighbors have been in the focus of different experimental campaigns. At REX-ISOLDE, ^{68}Ni has been studied through low-energy Coulomb excitation [22], by two-neutron transfer reaction $^{66}Ni(t,p)^{68}$Ni [23] and as a by-product in Mn decay studies [21]. The low-spin level scheme of the ^{68}Ni has also recently been investigated by A. Dijon *et al.* using the 6.3 MeV/u $^{70}Zn + ^{238}U$ reaction [24]. They proposed a third 0^+ isomeric state at 2202 keV on the basis of the observation of a 168 keV γ-ray. The non-observation of the 168 keV transition by C.J. Chiara *et al.* [25], in a similar reaction and using the Gammasphere array makes the assignment of this state unlikely. Angular correlation studies of γ-rays were performed and confirmed the spin/parity assignment of most of the already known levels, and specially for the 2511 keV 0^+ state. Further information on the level structure of ^{68}Ni comes from a study at Argonne of R. Broda *et al.* [1] using the $^{64}Ni + ^{238}U$ reaction.

In Fig. 2, the left panel shows the present experimental information of the low-spin level structure of ^{68}Ni. The position of the second 0^+ state is now firmly fixed at 1604 keV on the basis of the ^{68}Mn decay study at ISOLDE [21]. A description of the unpublished results will now be given as this also explains the improvements which are required. The setup used consisted of 3 plastic detectors and 2 MiniBall triple clusters in close geometry, surrounding the implantation point at the tape station. By using the coincidence relation between pairs of the three plastic detectors, 526 events were observed outside of the prompt coincidence window of two plastic detectors. Their time behavior is presented in Fig. 3 and fits well with the known half life of the first excited 0^+ state of 270 (5) ns [2]. These events are understood as the delayed coincidence between two plastic detectors.

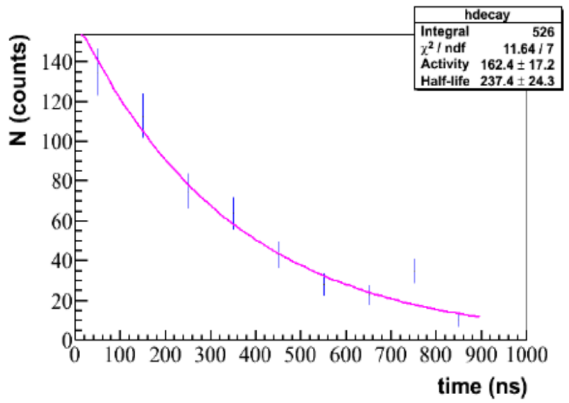

Figure 3: Time spectrum between two consecutive signals in the plastic detectors $[-1\mu s; +1\mu s]$, outside the prompt "$\beta - \beta$" time distribution (which corresponds to β-scattering from one detector to another). Courtesy of F. Flavigny [21].

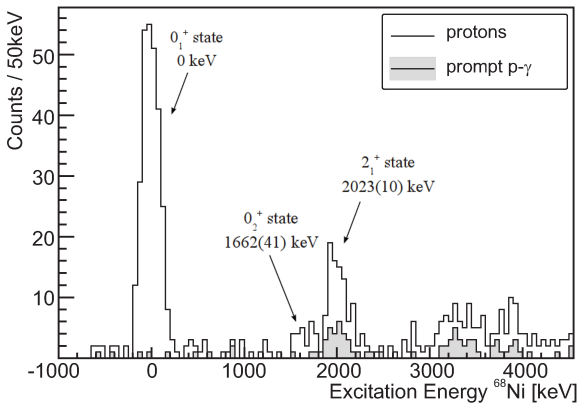

Figure 4: Excitation energy deduced from proton events of the $^{66}Ni(t,p)^{68}Ni$ transfer reaction. Courtesy of J. Elseviers [23].

Using this selective signal, it is possible to observe in the Ge detectors, the coincident gamma transitions built on top of the 0_2^+ state. Figure 5 shows this coincident spectrum and is understood as consisting of the 511 keV e^+ annihilation radiation from the pair creation and of the 1139 keV transition feeding. This line was observed in the previous decay study but its placement was unsure [6]. Also a 2421 keV line was observed in this spectrum and both gamma lines fit in the known level scheme fixing the energy of the first excited 0^+ state at 1604 keV, well below the earlier value of 1.77 (3) MeV [4, 5]. This year on a number of summer conferences and workshops, similar results on the position of the first excited 0^+ state were reported from recent ANL and MSU experiments [26].
In the $^{66}Ni(t,p)^{68}Ni$ transfer reaction at REX-ISOLDE feeding is observed to a level around 1.662(41) MeV with a weak strength of around 5% compared to the ground state (J. Elseviers Ph. D. work), see Fig. 4.

3 Proposed experimental goals

Figure 2a gives the present knowledge on transitions connecting the different 0^+ and 2^+ levels. Next to information from multi-step Coulomb excitation and transfer reactions (subject to another proposal) it is clear that crucial decay information is lacking, such as the β-feeding pattern, the intensity or upper limit of the yet unobserved transitions and the partial half-lives. In Fig. 2b, the calculated relative intensities of different E2 transitions are shown, based purely on the energy dependence of E2 transitions. The difference with the experimental values in Fig. 2a is striking and provides evidence for important nuclear-structure effects. In Fig. 2c, based on the $B(E2,\downarrow)^{theo.}$ transition strength taken from the thesis of A. Dijon [20] based on the LNPS calculations, also a number of relative intensities are given and a reasonable agreement with the experimental values is observed. Also a prediction of the a partial half-life of around 1.5 ns is proposed for the 478 keV transition from the 2511 keV level de-excitation. The determination of the 478 keV partial half-life is thus of great interest. Such half-lives are accessible via the fast-timing technique [27]. By tagging on the 1515 keV and 478 keV transitions, which respectively populate and depopulate the 2511 keV level, one could determine its half-life. The 478 keV transition could be in competition with the 2511 keV 0^+ to 0^+ transition which, based on the $\rho^2(E0)$ of the 1603.6 keV transition, would yield a partial half-life of 13 ns. Note however, that the $\rho^2(E0)$ value is very sensitive to the difference in deformation and mixing of the two 0^+ states [28] and it is thus not at all evident that 0^+_3 to 0^+_1 transition has the same strength as the 0^+_2 to 0^+_1 transition. The 2511 keV transition will mostly proceed by pair creation and give a signal in the plastic or Si detectors coincident with the 511 keV γ-rays.

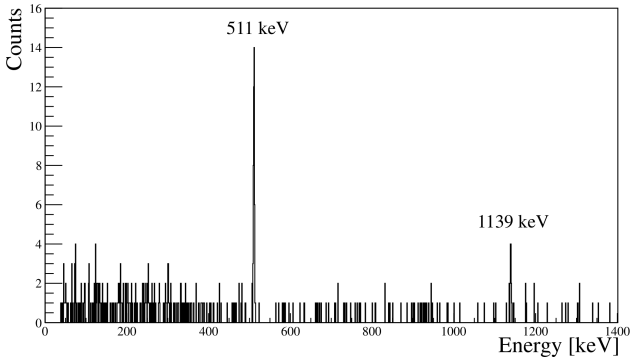

Figure 5: Energy spectrum of β^{prompt}-$\beta^{delayed}$-γ events. Courtesy of F. Flavigny and D. Radulov [21].

Strong and pure sources of the low-spin β-decaying state in ^{68}Co are populated in the decay of ^{68}Mn. The spin/parity of the isomeric state of 1.6 s ^{68}Co has been tentatively assigned to (1^+) by Liddick *et al.* [29] based on apparent strong feeding to the ground state. This is in conflict with the assignment of (3^+) by Mueller *et al.* [7]. Our recent decay study at ISOLDE does show apparent feeding to the 0^+, 2^+ states but also to the known 5^- isomeric state. However also strong feeding to high-lying states is observed. This puzzling situation can most probably be explained by pandemonium effects. Therefore a detailed measurement of the β-feeding pattern is needed and will shed light on the intriguing decay properties of the low-spin ^{68}Co isomer.

4 The Experimental Setup

We propose to separate the study of the low-lying 0^+ and 2^+ states in ^{68}Ni in two different campaigns, using two different configurations of the ISOLDE Decay Station at CERN. The first experiment will focus on the measurement of γ-rays and electrons in order to determine the branching ratios and on E0 transitions. The second experiment will be dedicated to the lifetime measurement of the third 0^+ state at 2511 keV.

Gamma and electron spectroscopy

The proposed experimental setup optimize considerably the efficiency of the high-resolution γ and charged particle detectors. A schematic view of the proposed IDS configuration is shown on Fig. 6a. In this setup, three high energy resolution HPGe clover detectors are positioned to cover a maximum of solid angle ($\Delta\Omega = 32\%$), surrounding the implantation point. The beam will be implanted onto a thin aluminized mylar tape. In order to disentangle the different branching ratios of low energy transitions, we envisage to use a

chamber of silicon detectors. The total β or electron-detection efficiency is estimated to be $\sim$ 60%. This setup will allow us to perform an accurate measurement of the electrons from E0 transitions linking 0^+ states and branching ratios. The data acquisition system will be used in trigger-less mode, which means that each event acquires a time stamp during the data recording. Additional treatment of the data will be carried out off-line.

The identification of the isomers can be achieved thanks to the combination of β- and γ-detection, using the "slow correlation technique" described in detail in Ref. [30]. While the design of the electron detector chamber is not yet settled, experience present in the collaboration for constructing similar chambers, e.g. the setup used at the RITU separator (JYFL), should guarantee a successful development.

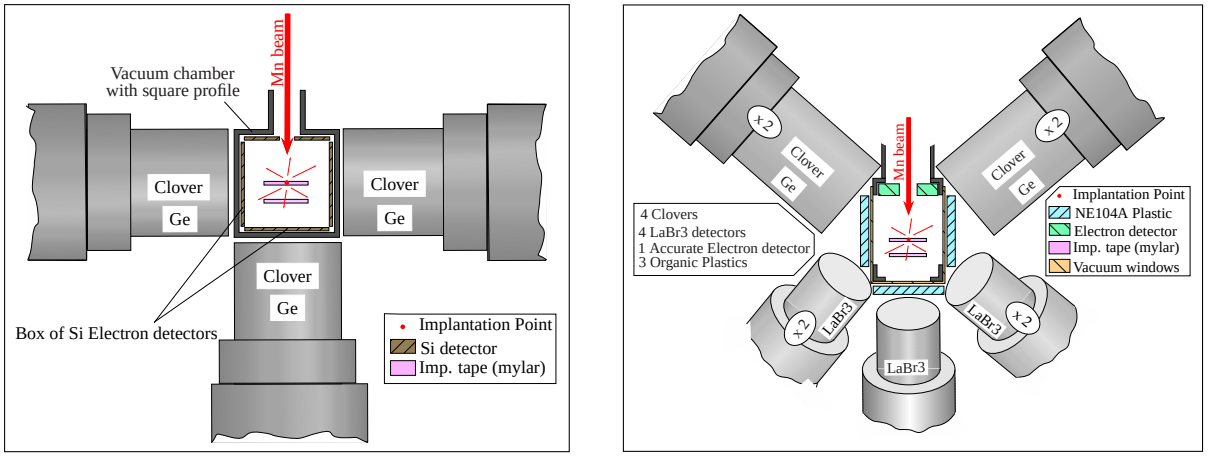

(a) Experimental setup for the measurement of gammas and electrons to determine the branching ratios and E0 components.

(b) Experimental setup for the measurement of the half-life of the third 0^+ state at 2511 keV.

Figure 6: Schematic view of the experimental setups. (not to scale)

Lifetime measurement

A representation of the experimental setup is shown on Fig. 6b. In order to determine the lifetime of the 0_3^+ isomeric state at 2511 keV, we will use the fast-timing technique. It can be achieved using $LaBr_3$ detectors ($\Delta\Omega = 14.4\%$) which possess a high time resolution. Three plastic detectors covering a solid angle of 60% will be used to trigger on the charged particles (β, E0 electrons). Four HPGe clover detectors ($\Delta\Omega \sim 20\%$) can be employed to clean the coincident spectra by tagging on γ-rays thanks to their high energy resolution.

5 Yields and Beam Time Request

As the direct production of Co isotopes is hampered at ISOLDE, pure sources of the low-spin isomer of ^{68}Co ($T_{1/2}$=1.6 s) will be obtained in the decay chain of ^{68}Mn($T_{1/2}$=28(4) ms) - ^{68}Fe($T_{1/2}$=132(39) ms). The Mn isotopes are produced with a UC_x target, a neutron converter and selective laser ionization. The laser ionization efficiency with the RILIS setup [31] of $\sim$19% is one of the highest obtained among the nuclei produced by ISOLDE.

Gamma and electron spectroscopy

To calculate the expected count rates in a total running time of 12 shifts, we assume a 2 μA proton beam and a transmission of 86% from primary target to tape station. Yields from the primary target are taken from the ISOLDE yield database [32] and on the previous Mn β-decay experiment performed at ISOLDE. The implantation yield has been determined to be 5.5 pps, which is in reasonable agreement with the 2 pps extracted from the decay study performed at ISOLDE close to the end of the target life cycle.
In the gamma and electron spectroscopy experiment, a limit of the number of E0 transitions associated to the 1603.6 keV level are expected to be $\sim$ 4.6 kCts/shift, based on the relative intensities of the 1139.0 keV and 2420.8 keV gamma transitions feeding the 1603.6 keV 0^+ level and the absolute feeding of the 2033.0 keV level (68%). The proportion of conversion electron/pair creation has been estimated to be 55%/45% from [33].

^{A}X	Energy [keV]	single γ_{HPGe} [Cts] /shift	β-γ_{HPGe} [Cts] Exp.
^{68}Ni	1515	444	3200
	478	1083	7800
	1139	302	2178
	2033	2778	20002

Table 1: SPECTROSCOPY SETUP. The count rates estimated for the ^{68}Ni lines are based on the relative intensities to the 2033 keV line observed in the 2009 ^{68}Mn decay study at ISOLDE. The latter are scaled on the absolute feeding of the 2033 keV level determined to be $\sim$ 68(10)% as deduced from our previous decay study. The total beta efficiency amounts to 60%.

The intensity of the E0 transitions from the 0_3^+ level at 2511 keV (towards the 0_2^+ and 0_1^+ states) will depend on the B(E2) value of the 478 keV transition (see Fig. 2c) and the expected $\rho^2(E0)$ strength. Taking the theoretical prediction for the B(E2) for the 478 keV transition and the $\rho^2(E0)$ strength of the 0_2^+-0_1^+ transition scaled with the energy factor, one expects a 10.3% and 0.079% for the E0 transition towards the 0_1^+ and 0_2^+, respectively. The former will essentially decay via pair creation and we expect 1374 Cts in the beta-gated electron 745.5 keV-511 keV gamma gate. Using the same assumptions, the 0_3^+-0_2^+ 906 keV E0 transition intensity will have $\sim$48 counts.

For the weakest gamma transition of interest (234 keV 2_2^+-0_3^+) the γ-ray intensity relative to the 2033 keV transition is expected to be 0.16% (see Fig. 2), which would result in 124 counts.

LIFETIME MEASUREMENT

For the lifetime measurement setup, the expected yields are summarized in Table 2 based on 12 shifts running.

^{A}X	Energy [keV]	single γ_{HPGe} [Cts] /shift	single γ_{LaBr_3} [Cts] /shift	β-γ_{LaBr_3} [Cts] Exp.
^{68}Ni	1515	254	62	447
	478	619	370	2663
	1139	173	40	286
	2033	1587	388	2794

Table 2: LIFETIME MEASUREMENT SETUP. The count rates estimated for the ^{68}Ni lines are based on the relative intensities to the 2033 keV line observed in the 2009 ^{68}Mn decay study at ISOLDE. The latter are scaled on the absolute feeding of the 2033 keV level determined to be $\sim$ 68(10)% as deduced from our previous decay study. The total beta efficiency amounts to 60%.

In order to determine the lifetime of the 2511-keV state, expected to be about 1.5 ns or longer, the statistics in the γ_{LaBr_3}(478)-γ_{LaBr_3}(1515) will most likely not suffice. But according to the estimated count rates, the amount of β-γ_{LaBr_3}(478) coincidences would be sufficient to determine the lifetime of the 2511-keV level by gating on the 478 keV transition. The resolution of the $LaBr_3$ ($\sim$25 keV at 500 keV) allows to resolve the 478-keV and 511-keV transitions. The time spectrum can be further cleaned by selecting a coincidence with the 1515-keV in the Ge detectors, at the expense of low statistics, of the order of 50 Cts in the complete experiment.

The Ga contaminant has a long half-life compared to the time sequence of the Mn-Fe-Co decay chain. By using the tape station, the unwanted activity at the experimental setup can also be reduced. Moreover, because of the short-half life of ^{68}Mn ($T_{1/2}$=28 ms), a short beam gate can be used which will further reduce the presence of ^{68}Ga at the implantation point.

In addition, to perform a proper selection of the observed γ-rays, a sufficient amount of laser-off data needs to be taken.

Thus, we would need 4 shifts dedicated to the optimization of the beam parameters and 12 shifts for each campaign. In total, we ask for **28 shifts** to perform the β-decay studies of the low-spin isomer of ^{68}Co, populated in the decay of ^{68}Mn, to obtain spectroscopic information on ^{68}Ni.

Summary of requested shifts: 2 shifts for optimization of beam settings, **12 shifts** for the measurement of branching ratios and E0 component of ^{68}Ni, another **2 shifts** for optimization, **12 shifts** for the lifetime measurement of the third 0^+ state of ^{68}Ni, which adds up to **28 shifts**.

References

[1] R. Broda et al., Phys. Rev. Lett. **74**, 868 (1995).

[2] O. Sorlin et al., Phys. Rev. Lett. **88**, 092501 (2002).

[3] M. Bernas et al., Physics Letters B **113**, 279 (1982).

[4] M. Girod et al., Phys. Rev. C **37**, 2600 (1988).

[5] M. Hannawald et al., Phys. Rev. Lett. **82**, 1391 (1999).

[6] W. F. Mueller et al., Phys. Rev. C **61**, 054308 (2000).

[7] W. F. Mueller et al., Phys. Rev. Lett. **83**, 3613 (1999).

[8] A. F. Lisetskiy, B. A. Brown, M. Horoi, and H. Grawe, Phys. Rev. C **70**, 044314 (2004).

[9] K. Langanke, J. Terasaki, F. Nowacki, D. J. Dean, and W. Nazarewicz, Phys. Rev. C **67**, 044314 (2003).

[10] K. Kaneko, M. Hasegawa, T. Mizusaki, and Y. Sun, Phys. Rev. C **74**, 024321 (2006), (Erratum: PRC 74, 4,049901,2006).

[11] M. Honma, T. Otsuka, T. Mizusaki, and M. Hjorth-Jensen, Phys. Rev. C **80**, 064323 (2009).

[12] N. Shimizu et al., Progress of Theoretical and Experimental Physics **2012** (2012).

[13] Y. Tsunoda, T. Otsuka, N. Shimizu, M. Honma, and Y. Utsuno, Journal of Physics: Conference Series **445**, 012028 (2013).

[14] K. Sieja and F. Nowacki, Phys. Rev. C **85**, 051301 (2012).

[15] T. Otsuka, M. Honma, T. Mizusaki, N. Shimizu, and Y. Utsuno, Progress in Particle and Nuclear Physics **47**, 319 (2001).

[16] D. Pauwels et al., Phys. Rev. C **82**, 027304 (2010).

[17] S. M. Lenzi, F. Nowacki, A. Poves, and K. Sieja, Phys. Rev. C **82**, 054301 (2010).

[18] D. Pauwels et al., Phys. Rev. C **78**, 041307 (2008).

[19] T. Otsuka, private communication, 2013.

[20] A. Dijon, *Evolution de la collectivité autour du ^{68}Ni: rôle des états intrus*, PhD thesis, l'Université de Caen, 2012.

[21] F. Flavigny and D. Radulov, β-decay studies of neutron rich $^{61-70}$Mn isotopes with the new LISOL β-decay setup, Technical report, CERN, 2013, private communication.

[22] N. Bree et al., Phys. Rev. C **78**, 047301 (2008).

[23] J. Elseviers, private communication, Ph D. work on the basis of the CERN-INTC-P-367 experiment.

[24] A. Dijon et al., Phys. Rev. C **85**, 031301 (2012).

[25] C. J. Chiara et al., Phys. Rev. C **86**, 041304 (2012).

[26] F. R. *at al.*, Configuration mixing and relative transition rates between low-spin states in ^{68}Ni, rapid communication, accepted, 2013.

[27] N. Mărginean et al., The European Physical Journal A **46**, 329 (2010).

[28] J. Wood, E. Zganjar, C. D. Coster, and K. Heyde, Nuclear Physics A **651**, 323 (1999).

[29] S. N. Liddick et al., Phys. Rev. C **85**, 014328 (2012).

[30] D. Pauwels et al., Nuclear Instruments and Methods in Physics Research Section B: Beam Interactions with Materials and Atoms **266**, 4600 (2008).

[31] V. Mishin et al., Nuclear Instruments and Methods in Physics Research Section B: Beam Interactions with Materials and Atoms **73**, 550 (1993).

[32] ISOLDE collaboration, CERN, Isolde yields database, 2013.

[33] T. Kibédi, T. Burrows, M. Trzhaskovskaya, P. Davidson, and C. N. Jr., Nuclear Instruments and Methods in Physics Research Section A: Accelerators, Spectrometers, Detectors and Associated Equipment **589**, 202 (2008).

Appendix

DESCRIPTION OF THE PROPOSED EXPERIMENT

The experimental setup comprises: (*name the fixed-ISOLDE installations, as well as flexible elements of the experiment*)

Part of the	Availability	Design and manufacturing
(if relevant, name fixed ISOLDE installation: COLLAPS, CRIS, ISOLTRAP, MINIBALL + only CD, MINIBALL + T-REX, NICOLE, SSP-GLM chamber, SSP-GHM chamber, or WITCH)	⊠ Existing	⊠ To be used without any modification
[Part 1 of experiment/ equipment]	□ Existing	□ To be used without any modification □ To be modified
	□ New	□ Standard equipment supplied by a manufacturer □ CERN/collaboration responsible for the design and/or manufacturing
[Part 2 of experiment/ equipment]	□ Existing	□ To be used without any modification □ To be modified
	□ New	□ Standard equipment supplied by a manufacturer □ CERN/collaboration responsible for the design and/or manufacturing
[insert lines if needed]		

HAZARDS GENERATED BY THE EXPERIMENT (if using fixed installation:) Hazards named in the document relevant for the fixed [COLLAPS, CRIS, ISOLTRAP, MINIBALL + only CD, MINIBALL + T-REX, NICOLE, SSP-GLM chamber, SSP-GHM chamber, or WITCH] installation.

Additional hazards:

Hazards	[Part 1 of experiment/ equipment]	[Part 2 of experiment/ equipment]	[Part 3 of experiment/ equipment]
Thermodynamic and fluidic			
Pressure	[pressure][Bar], [volume][l]		
Vacuum			
Temperature	[temperature] [K]		
Heat transfer			
Thermal properties of materials			
Cryogenic fluid	[fluid], [pressure][Bar], [volume][l]		
Electrical and electromagnetic			
Electricity	[voltage] [V], [current][A]		
Static electricity			
Magnetic field	[magnetic field] [T]		
Batteries	□		
Capacitors	□		
Ionizing radiation			
Target material [material]			
Beam particle type (e, p, ions, etc)			
Beam intensity			
Beam energy			
Cooling liquids	[liquid]		
Gases	[gas]		
Calibration sources:	□		

• Open source	□		
• Sealed source	□ [ISO standard]		
• Isotope			
• Activity			
Use of activated material:			
• Description	□		
• Dose rate on contact and in 10 cm distance	[dose][mSV]		
• Isotope			
• Activity			
Non-ionizing radiation			
Laser			
UV light			
Microwaves (300MHz-30 GHz)			
Radiofrequency (1-300 MHz)			
Chemical			
Toxic	[chemical agent], [quantity]		
Harmful	[chem. agent], [quant.]		
CMR (carcinogens, mutagens and substances toxic to reproduction)	[chem. agent], [quant.]		
Corrosive	[chem. agent], [quant.]		
Irritant	[chem. agent], [quant.]		
Flammable	[chem. agent], [quant.]		
Oxidizing	[chem. agent], [quant.]		
Explosiveness	[chem. agent], [quant.]		
Asphyxiant	[chem. agent], [quant.]		
Dangerous for the environment	[chem. agent], [quant.]		
Mechanical			
Physical impact or mechanical energy (moving parts)	[location]		
Mechanical properties (Sharp, rough, slippery)	[location]		
Vibration	[location]		
Vehicles and Means of Transport	[location]		
Noise			
Frequency	[frequency],[Hz]		
Intensity			
Physical			
Confined spaces	[location]		
High workplaces	[location]		
Access to high workplaces	[location]		
Obstructions in passageways	[location]		
Manual handling	[location]		
Poor ergonomics	[location]		

Hazard identification:

Average electrical power requirements (excluding fixed ISOLDE-installation mentioned above): [make a rough estimate of the total power consumption of the additional equipment used in the experiment]